

## ORIGINAL RESEARCH ARTICLE



# Personalized Heart Digital Twins Detect Substrate Abnormalities in Scar-Dependent Ventricular Tachycardia

Michael C. Waight<sup>1</sup>, MBBS, BSc(Hons), MRCP; Adityo Prakosa<sup>2</sup>, PhD; Anthony C. Li<sup>3</sup>, MD (Res), MBBS, BSc(Hons), MRCP; Nick Bunce, MD, MBBS, BSc, MRCP; Anna Marciniak, MBBS, PhD, MRCP; Natalia A. Trayanova<sup>4</sup>, PhD\*; Magdi M. Saba<sup>5</sup>, MD, MSc\*

**BACKGROUND:** Current outcomes from catheter ablation for scar-dependent ventricular tachycardia (VT) are limited by high recurrence rates and long procedure durations. Personalized heart digital twin technology presents a noninvasive method of predicting critical substrate in VT, and its integration into clinical VT ablation offers a promising solution. The accuracy of the predictions of digital twins to detect invasive substrate abnormalities is unknown. We present the first prospective analysis of digital twin technology in predicting critical substrate abnormalities in VT.

**METHODS:** Heart digital twin models were created from 18 patients with scar-dependent VT undergoing catheter ablation. Contrast-enhanced cardiac magnetic resonance images were used to reconstruct finite-element meshes, onto which regional electrophysiological properties were applied. Rapid-pacing protocols were used to induce VTs and to define the VT circuits. Predicted optimum ablation sites to terminate all VTs in the models were identified. Invasive substrate mapping was performed, and the digital twins were merged with the electroanatomical map. Electrogram abnormalities and regions of conduction slowing were compared between digital twin-predicted sites and nonpredicted areas.

**RESULTS:** Electrogram abnormalities were significantly more frequent in digital twin-predicted sites compared with nonpredicted sites (468/1029 [45.5%] versus 519/1611 [32.2%];  $P < 0.001$ ). Electrogram duration was longer at predicted sites compared with nonpredicted sites ( $82.0 \pm 25.9$  milliseconds versus  $69.7 \pm 22.3$  milliseconds;  $P < 0.001$ ). Digital twins correctly identified 21 of 26 (80.8%) deceleration zones seen on isochronal late activation mapping.

**CONCLUSIONS:** Digital twin-predicted sites display a higher prevalence of abnormal and prolonged electrograms compared with nonpredicted sites and accurately identify regions of conduction slowing. Digital twin technology may help improve substrate-based VT ablation.

**REGISTRATION:** URL: <https://www.clinicaltrials.gov>; Unique identifier: NCT04632394.

**Key Words:** catheter ablation ■ electrophysiologic techniques, cardiac ■ magnetic resonance imaging ■ tachycardia, ventricular

## Editorial, see p 534

Catheter ablation for scar-dependent ventricular tachycardia (VT) is an established treatment that has been proved to reduce defibrillator shocks and to prevent recurrence of arrhythmia in randomized controlled trials.<sup>1–3</sup> During ablation, the optimum outcome

is to induce and map the clinical VT to prove the location of the critical isthmus and to confirm its noninducibility after ablation.<sup>4,5</sup> However, sustained VT is frequently not hemodynamically tolerated, necessitating an alternative ablation strategy, known as substrate ablation, which

Correspondence to: Michael C. Waight, MBBS, BSc(Hons), MRCP, City St. George's, University of London, Cranmer Terrace, London, SW17 0RE. Email [m2110065@citystgeorges.ac.uk](mailto:m2110065@citystgeorges.ac.uk)

\*N.A. Trayanova and M.M. Saba contributed equally.

Supplemental Material is available at <https://www.ahajournals.org/doi/suppl/10.1161/CIRCULATIONAHA.124.070526>.

For Sources of Funding and Disclosures, see page 531.

© 2025 The Authors. *Circulation* is published on behalf of the American Heart Association, Inc., by Wolters Kluwer Health, Inc. This is an open access article under the terms of the [Creative Commons Attribution License](https://creativecommons.org/licenses/by/4.0/), which permits use, distribution, and reproduction in any medium, provided that the original work is properly cited.

*Circulation* is available at [www.ahajournals.org/journal/circ](http://www.ahajournals.org/journal/circ)

## Clinical Perspective

### What Is New?

- Magnetic resonance imaging–based heart digital twins were created from patients with scar-dependent ventricular tachycardia (VT) to assess their accuracy in detecting critical substrate abnormalities during VT ablation.
- The invasive electrophysiological properties of sites predicted to be of importance in sustaining VT by heart digital twins have not been studied previously.
- The personalized heart digital twins accurately detected both substrate and functional abnormalities during invasive VT ablation.

### What Are the Clinical Implications?

- Digital twin technology may improve efficacy and act as a guide for catheter ablation of ventricular tachycardia.
- Using digital twins in VT ablation may help reduce procedure time, complications, and length of hospital stay in the future.

## Nonstandard Abbreviations and Acronyms

<b>3D</b>	3-dimensional
<b>DZ</b>	deceleration zone
<b>EAM</b>	electroanatomic map
<b>EGM</b>	electrogram
<b>ICM</b>	ischemic cardiomyopathy
<b>LGE-CMR</b>	late gadolinium-enhanced cardiac magnetic resonance imaging
<b>LV</b>	left ventricular
<b>MRI</b>	magnetic resonance imaging
<b>NICM</b>	nonischemic cardiomyopathy
<b>VT</b>	ventricular tachycardia

is principally targeted toward the elimination of abnormal electrograms (EGMs) seen in and around the area of myocardial scar. Techniques include abolition of late potentials,<sup>6</sup> local abnormal ventricular activity,<sup>7</sup> and scar homogenization.<sup>8</sup> Despite evidence that VT ablation can effectively treat VT,<sup>9</sup> long-term recurrence rates in recent large trials are between 31% and 48%.<sup>10–12</sup> Procedure-related complications are frequent,<sup>13</sup> and ablations can last several hours.<sup>14</sup> Therefore, there is a requirement to make VT ablation safer, faster, and more effective.

A digital twin is a virtual representation of a system that mimics the structure and function of the system and has a predictive capability, informing decisions that real-time value.<sup>15</sup> Medical digital twins, which are computational models of organs (and even patients) created with patient data, have been making significant inroads in medicine to support clinical decision-making.<sup>16</sup> Heart digital twins,

which are personalized mechanistic computational models of patient hearts constructed from patient data that represent the functioning of the patient heart, have been used for a number of clinical applications in recent years.<sup>17</sup> They have demonstrated accurate prediction of risk of sudden cardiac death in both ischemic and nonischemic populations<sup>18–21</sup> by evaluating the arrhythmogenic propensity of the disease-remodeled (fibrotic or scarred) myocardial milieu. Heart digital twins incorporating genetic predisposition<sup>19</sup> or penetrating adiposity<sup>22,23</sup> have recently been used to predict the locations of VT circuits. Heart digital twins have been proposed as the technology that could predict noninvasively, before the procedure, the optimal personalized targets in patients undergoing VT ablation,<sup>24</sup> directly guiding the delivery of lesions that fully eliminate the likelihood of arrhythmia occurrence. Should this technology become clinical reality, it would potentially improve procedural success, reduce the risk of long-term arrhythmia recurrence, and allow a shorter, more targeted, ablation procedure, thereby reducing complications and length of hospital stay. However, to achieve the full potential of digital twins in improving VT ablation, the technology needs to be evaluated intraprocedurally in the cardiac electrophysiology laboratory, and its agreement with invasive recordings of patient's electrophysiological activity should be demonstrated. The invasive electrophysiological characteristics of these digital twin–predicted arrhythmogenic sites have not been studied previously.

We present the first combined prospective clinical and heart digital twin study with the aim of invasively evaluating the accuracy of the personalized model predictions. Specifically, we construct heart digital twins in a cohort of patients with ischemic cardiomyopathy (ICM) and nonischemic cardiomyopathy (NICM) undergoing ablation for scar-dependent VT and to predict the substrate locations most likely to sustain reentrant arrhythmias. We examine digital twin arrhythmogenesis arising both in the native substrate and in the postablation substrate, an approach that is unique to our personalized prediction of VT ablation targets. During clinical VT ablation, we perform comprehensive substrate mapping and evaluate EGM properties at sites deemed to be of critical importance by the digital twin to establish their relation to the conventional substrate-mapping approach to VT ablation. Ascertaining the capabilities of the heart digital twins to predict optimal targets for scar-related VT would open the door to novel means of delivering treatment to patients with VT and thus chart a pathway for the personalized management of ventricular arrhythmia.

## METHODS

### Data Availability

Mesh geometries and simulation data are available on reasonable request (to N.A.T.). Patient data used in this study cannot be made publicly available without further consent and ethical approval because of privacy concerns. Magnetic resonance imaging (MRI) images can be provided by the authors pending

St. George's Hospital Medical Imaging Department approval and a completed material transfer agreement. Codes for image processing and simulations are available on reasonable request to the corresponding author.

## Study Overview

This was a single-center prospective study with 2 phases. First, consecutive patients with scar-dependent VT requiring catheter ablation prospectively underwent late gadolinium-enhanced cardiac MRI (LGE-CMR). From each image, we generated a heart digital twin reflecting the distribution of the patient's scar. Next, arrhythmia inducibility after pacing was tested in the digital twin to determine the optimum ablation sites to terminate all possible VTs in the model. Subsequently, the patient underwent invasive VT ablation that included comprehensive substrate mapping. During VT ablation, the digital twin and the clinical electroanatomical map (EAM) were merged. EGM abnormalities were compared between sites predicted by the heart digital twin to be of importance and nonpredicted sites, and the correspondence was evaluated. Figure 1 presents an overview of the study.

## Patient Population

Consecutive patients with scar-dependent VT in the setting of both ICM and NICM requiring catheter ablation were prospectively recruited. Indications for catheter ablation included recurrent VT or implantable cardioverter defibrillator therapy, prohibitive side effects, or unwillingness to take antiarrhythmic drugs. All patients described in this study provided written informed consent. The study was approved by the Health Research Authority London–Surrey Research Ethics Committee (21/LO/0083). This study was registered at URL: [www hyperlink]HYPERLINK "http://www.clinicaltrials.gov"[www hyperlink] www.clinicaltrials.gov; Unique identifier: NCT04632394.

## Cardiac MRI Protocol

Patients underwent preprocedural LGE-CMR, including a 3-dimensional (3D) LGE sequence. Details of image acquisition are provided in the [Supplemental Methods](#). Briefly, LGE-CMR was performed with a 3-T Philips Achieva for patients without implantable cardiac devices and a 1.5-T Siemens Magnetom Aera (with wideband sequences) for those with devices. LGE-CMR images were acquired with a free-breathing respiratory-navigated sequence with an image resolution of  $1.3 \times 1.3 \times 1.8$  mm. Only patients with sufficient MRI quality were included, defined as having the entire left ventricular (LV) myocardium visible within the MRI field of view, with clearly identifiable scar boundaries and the absence of artifact affecting the scar region.

## Generation of the Heart Digital Twin

Acquired 3D LGE-CMR images were used as the basis for the generation of a heart digital twin (a personalized mechanistic computational model) for each patient that represented the electrical functioning of the patient's heart. The digital twin was used to induce VTs, to define their circuits, and to derive optimum ablation lesion sets that terminate all VTs that a patient's digital twin can sustain. This methodology has been described in detail in previous publications from our group and is outlined in the [Supplemental Methods](#).<sup>22,24–26</sup>

## Construction of a Patient's Heart Geometric Model

Endocardial and epicardial boundaries from the 3D LGE-CMR images are contoured, and the myocardium is categorized as dense scar, border zone, or healthy tissue with a validated full-width half-maximum approach.<sup>27</sup> Finite-element meshes with an average resolution of  $400 \mu\text{m}$  were generated, containing

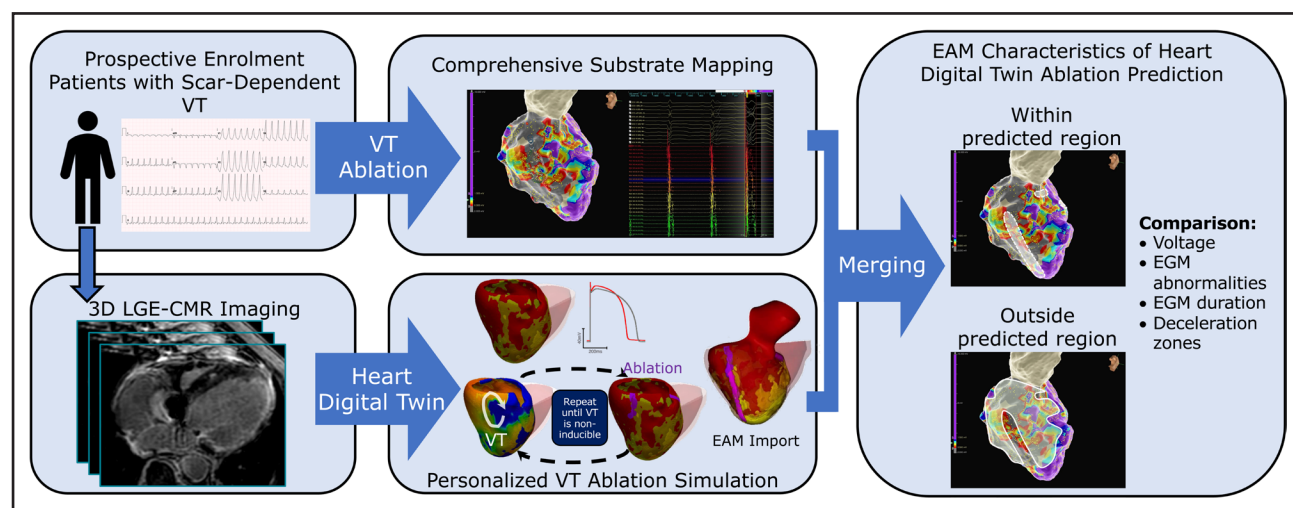


**Figure 1. Study overview.**

Prospective patients with scar-dependent ventricular tachycardia (VT) were recruited and underwent high-quality 3-dimensional late gadolinium-enhanced cardiac magnetic resonance (3D LGE-CMR; **left**). Patients underwent personalized cardiac digital twin creation (**middle, bottom**) with iterative VT induction and ablation to reveal and terminate all VTs, including postablation emergent arrhythmias. Patients also underwent comprehensive substrate mapping (**middle, top**) and invasive VT ablation. Digital twin predictions were merged with the substrate map for comparison of substrate abnormalities digital twin–predicted sites and sites outside the predicted regions (**right**). EAM indicates electroanatomical map; and EGM, electrogram.

≈4 million individual nodes.<sup>28</sup> Fiber direction was subsequently applied to the mesh.<sup>29</sup>

## Application of Electrophysiological Properties to the Model

Electrophysiological properties were applied to each of the 3 tissue regions in the patient's heart digital twin. Dense scar was modeled as electrically inert. Healthy tissue was assigned ventricular action potential kinetics with the Ten Tusscher et al<sup>30</sup> ionic model. Border zone was assigned modified kinetics, characterized by a slower action potential upstroke velocity, reduced peak amplitude, longer action potential duration, and reduced cell-cell conductivity.<sup>20</sup> Wavefront propagation was simulated by solving the reaction-diffusion partial differential equation using the open-source software openCARP (<https://opencarp.org>) on a parallel computing system.<sup>31</sup>

## Simulated Pacing and Ablation Protocol

To test VT inducibility in the digital twin, simulated pacing was applied from 7 LV sites based on a condensed 17-segment American Heart Association model, preferentially delivered to sites of border zone to maximize the likelihood of inducing reentry. Pacing was delivered as a train of 6 beats at a cycle length of 600 milliseconds (S1), followed by up to 4 premature extrastimuli until VT was observed.<sup>20,23,24</sup>

## Ablation in Heart Digital Twins

### Application of Simulated Ablation Lesions at Primary Sites

Once reentry was identified in the digital twin, each VT was analyzed for critical sites, including the entrance, isthmus, and exit. Simulated ablation lesions were applied to the VT isthmus to terminate reentry in that location. Simulated ablation lesions have a radius of 3.5 mm and are assumed to be transmural. When feasible, ablation lesions were extended from the isthmus to connect to adjacent regions of nonconducting, transmural dense scar, or anatomical barriers. This was done to avoid the emergence of secondary, iatrogenic VTs after ablation. These lesion sets were subsequently modeled as insulators. Lesions applied to the original substrate during this first round of simulation were labeled primary sites.

### Repeat Simulation and Secondary Site Identification

After application of primary site ablation lesions, the VT induction and ablation protocol was repeated to assess VT inducibility in the postablation substrate, consisting of the residual native scar and ablation lesions. If new VTs emerged, further ablation lesion sets were applied in a similar fashion to the primary sites and called secondary sites. The process was repeated until the patient's digital twin was no longer inducible to VT. This represents the hallmark of our digital twin approach and is designed to prevent the emergence of new VTs after the index ablation procedure, thus decreasing redo procedures and rehospitalizations.

Each predicted ablation lesion set typically terminated 1 VT but may be extended to also terminate a second VT circuit located in close proximity to the first. Predicted sites in our subsequent analysis were considered to be the primary and secondary ablation lesion sites that terminated all VTs during

the simulation. Sites of lesion extension to nearby nonconducting barriers to prevent iatrogenic VT were excluded for EGM analysis.

### Invasive VT Mapping and Ablation Protocol

After generation of the heart digital twin, patients underwent clinical VT ablation. Antiarrhythmic medications were discontinued 5 half-lives before ablation, with the exception of amiodarone, which was discontinued 1 week before ablation. Ablation was performed under general anesthesia. Epicardial access was gained at the operator's discretion as determined by cause and the presence of epicardial scar on CMR and in those presenting for redo ablation. When possible, dual LV access was gained through both the transeptal and retrograde aortic approaches. EAM was performed with the Ensite Precision or Ensite X systems and the multipolar Advisor HD Grid mapping catheter (Abbott Laboratories, Chicago, IL). Substrate mapping was performed during right ventricular pacing at 600 milliseconds for 3 beats followed by an extrastimulus (S2) at 20 milliseconds above ventricular effective refractory period. Standard low-voltage bipolar thresholds (0.5–1.5 mV endocardial, 0.5–1.0 mV epicardial) were applied.

After substrate mapping, VT was induced with programmed electrical stimulation and (if tolerated) mapped with activation and entrainment mapping to identify the critical isthmus and to guide ablation. If the VT was not hemodynamically tolerated, a substrate-based approach to ablation was used. The procedural end point was defined as noninducibility of all significant VTs after repeat programmed electrical stimulation.

### Integration of the Digital Twin With the EAM

Fiducial landmarks, including the left and right coronary cusps and the LV outflow tract from the digital twin, were aligned with their counterparts on the EAM once the full invasive geometry and substrate map had been created. Rigid merging of the 2 maps (digital twin and EAM) was performed with the Ensite Fusion Registration Module. Coregistration was performed by an expert independently of subsequent analysis who was blinded to predicted site location. Care was taken to achieve the closest merge possible in all 3 orthogonal planes. Operators were blinded to the location of the predicted sites or any of the digital twin surfaces at all times. The operators had access to the conventional LGE-CMR images preprocedurally, in line with current gold standard of care for VT ablation, to help guide the appropriate access routes.

### EGM Analysis

Acquired EGMs were analyzed on the Ensite mapping system and with a bespoke MATLAB Runtime. Measurements of EGM timing and morphological abnormalities were assessed by investigators blinded to location on the EAM and in accordance with accepted literature.<sup>7,32,33</sup> Parameters assessed include bipolar and unipolar voltage; QRS onset, offset, and duration; EGM onset, offset, and duration; and EGM morphological abnormalities. A full description of these abnormalities is given in [Table S1](#). [Figure S1](#) shows examples of these measurements and abnormalities.

Comparison of LV endocardial EGMs was made between predicted and nonpredicted sites at different tissue regions based on accepted voltage cutoffs, including dense scar (bipolar amplitude <0.5 mV), border zone (0.5–1.5 mV), and healthy tissue (>1.5 mV). EGM characteristics at primary predicted

sites (predicted by the digital twin to be responsible for VTs that arise in the native scar substrate) were compared with those of secondary sites (those predicted to arise de novo after ablation of the primary sites).

### Endocardial Scar Size Analysis

Comparison was made between the size of the low-voltage region on the EAM and the MRI-defined scar. Total endocardial bipolar and unipolar low-voltage area was calculated by contouring the area of low voltage according to accepted criteria (<1.5 mV bipolar, <8.3 mV unipolar) and compared with the area of MRI-defined scar.

### Functional Substrate Mapping Analysis

EGMs from extrastimulus pacing maps were analyzed, and EGM abnormalities were compared between predicted and nonpredicted sites. The increase in its duration in response to extrastimulus pacing was compared between predicted and nonpredicted regions. During right ventricular pacing, isochronal late activation maps were created with a previously described methodology.<sup>34,35</sup> Briefly, each EGM was annotated to the last deflection. The total LV activation window was divided into 8 colors (isochrones), each representing one-eighth of the total LV activation time. A deceleration zone (DZ) was defined as displaying >3 isochrones within a 1-cm radius. Spatial correlation of DZ with predicted areas was analyzed. A DZ within 5 mm of a predicted area, measured as geodesic distance, was considered spatially related to a predicted site. Analysis was performed for both primary and secondary digital twin-predicted sites.

### Statistical Analysis

Continuous, normally distributed data are expressed as mean±SD. Nonparametric data are expressed as median (interquartile range). Categorical data are expressed as total number and percentage. Linear mixed models were constructed to compare EGM abnormalities between predicted and nonpredicted sites, with patients as a random effect. Comparison of continuous, nonparametric data within individuals was done with Mann-Whitney *U* test. Categorical variables within individuals were compared with  $\chi^2$  tests. Receiver-operating characteristic curves were used to determine the optimum voltage cutoffs that correspond to MRI-defined scar. A value of  $P<0.05$  was taken to indicate statistical significance. Statistical analysis was carried out with SPSS version 30 (IBM Corp, Armonk, NY).

## RESULTS

### Patient Demographics

Thirty-seven patients with scar-dependent VT were screened, of whom 18 had sufficient-quality LGE-CMR images for heart digital twin creation. Seventeen of 18 (94.4%) were male. Baseline LV ejection fraction was  $42.3\pm 16.5\%$ . Those with NICM exhibited a higher baseline ejection fraction ( $46.3\pm 10.0\%$  versus  $41.5\pm 17.7\%$ ) compared with those with ICM. Seventeen of 18 (94.4%) were taking  $\beta$ -blockers; 7 of 18 (38.9%) were taking amiodarone; and three of 18 (16.7%) were taking mexiletine. All but 1 patient had either an implantable cardio-

verter defibrillator or cardiac resynchronization therapy-defibrillator in situ. Epicardial mapping was performed in 5 of 18 cases (27.8%). Table 1 shows the full baseline demographics of the cohort.

### Scar and Predicted Site Distribution and Comparison of Invasive and MRI-Defined Scar Size

Analysis of the distribution of the LGE area from the 3D CMR suggested a preponderance of inferior and lateral scars. Scar location was inferolateral in 5 of 18 cases (27.8%), lateral in 4 of 18 cases (22.2%), septal in 4 of 18 cases (22.2%), inferior in 3 of 18 cases (16.7%), and anterior in 2 of 18 cases (11.1%). During digital twin simulation, a total of 92 predicted sites were identified, including 62 primary and 30 secondary sites. All predicted sites were located within MRI scar. Sixty-five of 92 (70.7%) were located primarily within border zone, and 27 of 92 (29.3%) were primarily within dense scar. Average predicted site length and width were  $45.5\pm 40.3$  and  $8.08\pm 2.31$  mm, respectively. As shown in Figure 2A, there were no significant differences in the distribution of scar compared with predicted sites, confirming a correlation between scar location and the sites of the VT isthmus observable in the digital twins.

After coregistration of the digital twins with the EAMs, mean distance between the 2 surfaces was measured at  $3.95\pm 0.93$  mm. Table S2 shows the distance for each case between the EAM and the MRI. We next compared the area of low voltage on the EAM according to accepted cutoffs with the CMR LGE scar. On the EAM, median bipolar low-voltage (<1.5 mV) area was  $28.9$  cm<sup>2</sup> (21.8–41.3 cm<sup>2</sup>). Unipolar low-voltage (<8.3 mV) area was  $48.4$  cm<sup>2</sup> (32.8–59.2 cm<sup>2</sup>). On CMR, LGE scar area was  $46.1$  cm<sup>2</sup> (40.4–59.2 cm<sup>2</sup>). Unipolar low-voltage area and MRI scar area were significantly larger than bipolar low-voltage area ( $P=0.01$  and  $P=0.02$ , respectively); however, MRI scar area was not significantly different from unipolar scar area ( $P=0.89$ ), as shown in Figure 2B. Data on the discrepancy in scar size between EAM and MRI for each patient are given in Table S3. The data suggest a better correspondence between unipolar voltage mapping and the CMR-determined scar. Figure S2 shows an example of how the bipolar low-voltage area underestimated the scar size relative to the MRI, whereas the unipolar low-voltage area appeared more closely aligned. Receiver-operating characteristic curve analysis revealed an optimum for bipolar voltage in the detection of MRI LGE of 2.3 mV (area under the curve, 0.79 [0.78–0.79]), which is considerably higher than the traditional 1.5-mV threshold typically used.<sup>36</sup> Unipolar voltage receiver-operating characteristic curve analysis revealed an optimum cutoff of 7.9 mV (area under the curve, 0.78 [0.77–0.78]), which is more closely aligned to the accepted value of 8.3 mV.<sup>37</sup> Receiver-operating characteristic curves for this comparison are shown in Figure S3.

**Table 1. Baseline Demographics of the Cohort**

	ICM (n=15)	NICM (n=3)	Total (n=18)
Age, y	67.7±9.7	71.7±7.4	68.4±9.5
Male sex, n (%)	14 (93.3)	3 (100)	17 (94.4)
Baseline EF, %	41.5±17.7	46.3±10.0	42.3±16.5
NYHA class, n (%)			
I	7 (46.6)	1 (33.3)	8 (44.4)
II	5 (33.3)	2 (66.7)	7 (38.9)
III	3 (20.0)	0	3 (16.7)
IV	0	0	0
Hypertension, n (%)	11 (73.3)	2 (66.7)	13 (72.2)
Diabetes, n (%)	6 (40.0)	1 (33.3)	7 (38.9)
Atrial fibrillation, n (%)	6 (40.0)	2 (66.7)	8 (44.4)
Chronic kidney disease, n (%)	7 (46.7)	2 (66.7)	9 (50.0)
β-Blocker, n (%)	14 (93.3)	3 (100)	17 (94.4)
Amiodarone, n (%)	4 (26.7)	3 (100)	7 (38.9)
Mexiletine, n (%)	2 (13.3)	1 (33.3)	3 (16.7)
ICD, n (%)	12 (80.0)	3 (100)	15 (83.3)
CRT-D, n (%)	2 (10.7)	0	2 (11.1)
Prior VT ablation, n (%)	2 (13.3)	0	2 (11.1)
Prior cardiac surgery, n (%)	6 (40.0)	0	6 (33.3)
Epicardial mapping, n (%)	3 (16.7)	2 (66.7)	5 (27.8)

AAD indicates antiarrhythmic drug; CRT-D, cardiac resynchronization therapy–defibrillator; EAM, electroanatomical map; EF, ejection fraction; ICD, implantable cardioverter defibrillator; ICM, ischemic cardiomyopathy; NICM, nonischemic cardiomyopathy; NYHA, New York Heart Association; and VT, ventricular tachycardia.

### Comparison of EGM Abnormalities Between Predicted and Nonpredicted Sites Within Scar

Next, we compared EGM abnormalities between sites on the EAM that correspond to the predictions from the heart digital twin with nonpredicted sites. The median total number of EAM points per patient was 1512 (1287–2209). A total of 23 794 bipolar, endocardial LV EGMs were analyzed, of which 7699 were of low voltage (<1.5-mV bipolar amplitude), and 2640 points from within dense scar (<0.5-mV bipolar amplitude). Within dense scar, there was no difference in bipolar voltage between the predicted and nonpredicted sites (0.31±0.11 mV versus 0.32±0.11 mV;  $P=0.69$ ), suggesting that any differences between predicted and nonpredicted sites were not simply due to a greater extent of scar in these areas. All EGM abnormalities were more frequently seen in predicted areas compared with nonpredicted areas with the exception of double potentials. Overall, EGM abnormalities were seen in 468 of 1029 predicted sites (45.5%) versus 519 of 1611 nonpredicted sites (32.2%;  $P<0.001$ ). Measures of EGM timing differed significantly between predicted and nonpredicted sites, with predicted-site EGMs displaying longer total duration at 82.0±25.9 milliseconds compared with 69.7±22.3 milliseconds at nonpredicted sites ( $P<0.001$ ). Sensitivity and specificity

for detection of EGM abnormalities within dense scar were 45.8±23.6% and 71.1±24.6%, respectively. These results demonstrate the unusually high prevalence of EGM abnormalities at digital twin–predicted sites, establishing them as viable targets for ablation. Table 2 shows the comparison of EGM abnormalities identified at predicted and nonpredicted sites. Figure 3 shows several examples of invasively mapped substrate, the digital twin predictions, and the final ablation lesion set applied.

We then compared EGM characteristics at other tissue regions using accepted bipolar voltage cutoffs, including the border zone (0.5–1.5 mV) and healthy areas (>1.5 mV). At each region, predicted areas demonstrated increased frequency of EGM abnormalities and more prolonged EGM duration compared with voltage-matched, nonpredicted areas, as shown in Figure 4. Figure S4 shows a comparison of EGM duration and abnormalities between predicted and nonpredicted sites for each of the 18 cases in the study.

### Comparison of Substrate Abnormalities at Primary Versus Secondary Predicted Sites

To compare the differences between EGMs at digital twin–predicted primary and secondary sites, we undertook a subanalysis of the substrate at each site. The mean number of predicted sites was 5.3±1.8 per patient, comprising on average 3.5±1.2 primary sites and 1.8±1.3 secondary sites. Mean predicted area was 10.9±3.9 cm<sup>2</sup>, which constituted 22.2% (18.2%–34.6%) of the total scar area. Predicted-site area comprised 7.7±2.6 cm<sup>2</sup> from primary sites and 3.2±3.2 cm<sup>2</sup> from secondary sites. Six of 18 patients (33.3%) had no secondary predicted sites in the digital twins.

Within areas of low voltage (<1.5 mV), double potentials, late potentials, and other local abnormal ventricular activity were more frequent in primary compared with secondary sites. However, the prevalence of all EGM abnormalities combined did not differ significantly between primary and secondary sites, being present in 710 of 1748 primary sites (40.6%) versus 406 of 1074 secondary sites (37.8%;  $P=0.14$ ). There were no significant differences in measures of EGM timing between primary and secondary sites, with an overall EGM duration of 77.9±26.6 milliseconds at primary sites compared with 76.9±24.4 milliseconds at secondary sites ( $P=0.30$ ). These differences, summarized in Table 3, indicate that, from a substrate perspective, primary sites do not differ significantly from secondary sites.

### Evaluation of Functional Substrate Mapping at Digital Twin–Predicted Sites

We next assessed the electrophysiological parameters of predicted sites using 2 forms of functional substrate mapping: extrastimulus mapping to detect EGM prolongation

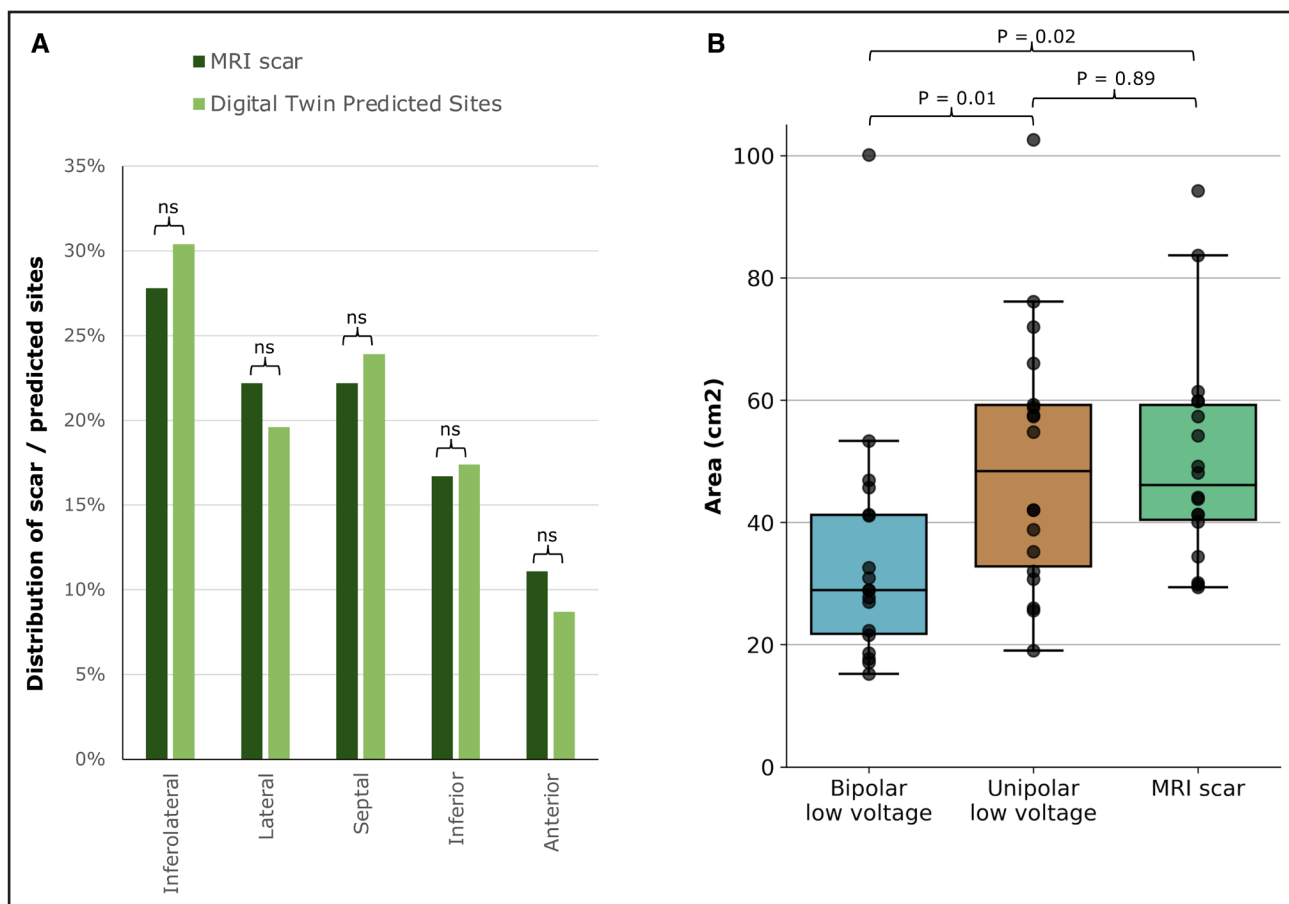


**Figure 2. Digital twin, electroanatomical scar, and MRI scar characteristics.**

**A.** Predominant left ventricular scar location and digital twin–predicted site location within the cohort. **B.** Comparison of bipolar low-voltage area, unipolar low-voltage area, and magnetic resonance imaging (MRI)–defined scar area. ns indicates not significant.

under stress and slow-conducting regions, as evidenced by DZs on isochronal late activation maps. In total, 6866 bipolar extrastimulus EGMs were analyzed. Abnormalities were observed in 1312 of 2773 predicted-site EGMs (47.3%) compared with 1116 of 4093 nonpredicted-site EGMs (27.3%;  $P < 0.001$ ). Mean EGM duration remained longer at predicted sites compared with nonpredicted sites ( $87.7 \pm 31.3$  milliseconds versus  $73.9 \pm 23.7$  milliseconds;  $P < 0.001$ ), and the average EGM prolongation in response to extrastimulus pacing was greater at predicted sites compared with nonpredicted sites ( $11.7 \pm 16.5$  milliseconds versus  $7.5 \pm 8.5$  milliseconds;  $P = 0.02$ ). These results indicate that the prediction sites of heart digital twins respond particularly poorly to conditions of stress, which is a hallmark of the critical VT isthmus.

On isochronal late activation mapping, a total of 26 DZs were identified, indicating regions of conduction slowing. There was a mean of  $1.44 \pm 1.20$  DZs per patient. Twenty-three of 26 (88.5%) were located on the endocardium, with 3 of 26 (11.5%) located on the epicardium. Twenty-one of 26 right ventricular paced DZs (80.8%) were located within 5 mm of a predicted site. The median geodesic distance from the center of the

DZ to the closest predicted area was 1 mm (range, 0–32 mm). Eighteen of the 26 DZs (69.2%) were located closest to a primary predicted site, whereas eight of 26 (30.8%) were located closest to a secondary predicted site. These results suggest that the digital twin predictions accurately detect regions of slow conduction, which are essential for the formation of reentry. Figure 5 shows a patient with ICM and lateral wall scar in whom isochronal late activation mapping revealed a DZ along the anterior edge of the low-voltage area. This corresponded to a predicted site from the patient's digital twin.

### VT Induction and Entrainment Mapping

After substrate mapping, monomorphic VT was inducible in 15 of 18 patients (83.3%). Two of 18 (11.1%) were not inducible to any ventricular arrhythmia, whereas 1 of 18 (5.6%) was inducible only for ventricular fibrillation. Because of hemodynamic instability in most patients, entrainment mapping was possible in only 4 of 18 cases (22.2%). In 3 of the 4 patients (75.0%), middiastolic activity during VT and entrainment with concealed fusion were found within 5 mm of a predicted site.

**Table 2. Comparison of Bipolar Voltage and EGM Characteristics From Within Areas of Dense Scar According to Accepted Cutoffs (Bipolar Voltage <0.5 mV) Between Predicted and Nonpredicted Sites**

Parameter	Predicted (n=1029)	Nonpredicted (n=1611)	P value
Voltage			
Bipolar voltage, mV	0.31±0.11	0.32±0.11	0.69
EGM characteristics, n (%)			
Fractionation	408/1029 (39.7)	435/1611 (27.0)	<0.001
Double potential	25/1029 (2.4)	24/1611 (1.5)	0.08
Late potential	40/1029 (3.9)	18/1611 (1.1)	<0.001
Other LAVA	86/1029 (8.4)	90/1611 (5.6)	0.01
Any EGM abnormality	468/1029 (45.5)	519/1611 (32.2)	<0.001
EGM timing, ms			
Onset	50.8±31.9	57.9±31.7	<0.001
Offset	132.8±26.9	127.5±25.0	<0.001
Duration	82.0±25.9	69.7±22.3	<0.001
Offset to QRS offset	33.1±28.0	36.1±27.8	0.01

EGM indicates electrogram; and LAVA, local abnormal ventricular activity.

## DISCUSSION

This study presents the first combined prospective heart digital twin and clinical study in which patients requiring

VT ablation undergo not only personalized arrhythmia simulation and prediction of optimum ablation lesions but also systematic analysis of the invasive electrophysiological substrate. This approach allowed comprehensive validation of the heart digital twins by identifying the characteristics of the prediction in relation to the substrate abnormalities and comparing them with bystander regions within the scar, demonstrating significant differences between the predicted and bystander regions. This study is crucial in demonstrating to electrophysiologists the emerging role of modeling-guided VT ablation and therefore serves as a bridge to bringing the routine use of heart digital twins in guiding VT ablation closer to reality.

## Prediction of Substrate Abnormalities

The main findings of this study are that the predictions of the digital twins of the critical targets for VT ablation exhibit greater EGM abnormalities during substrate mapping compared with voltage-matched, nonpredicted areas. Furthermore, EGM behavior in response to stress during functional substrate mapping was particularly abnormal at predicted sites compared with nonpredicted sites, and areas of conduction slowing, which are crucial for the establishment of reentry, frequently arose at these predicted sites. In a departure from other digital twin development studies, we include patients with both NICM and ICM

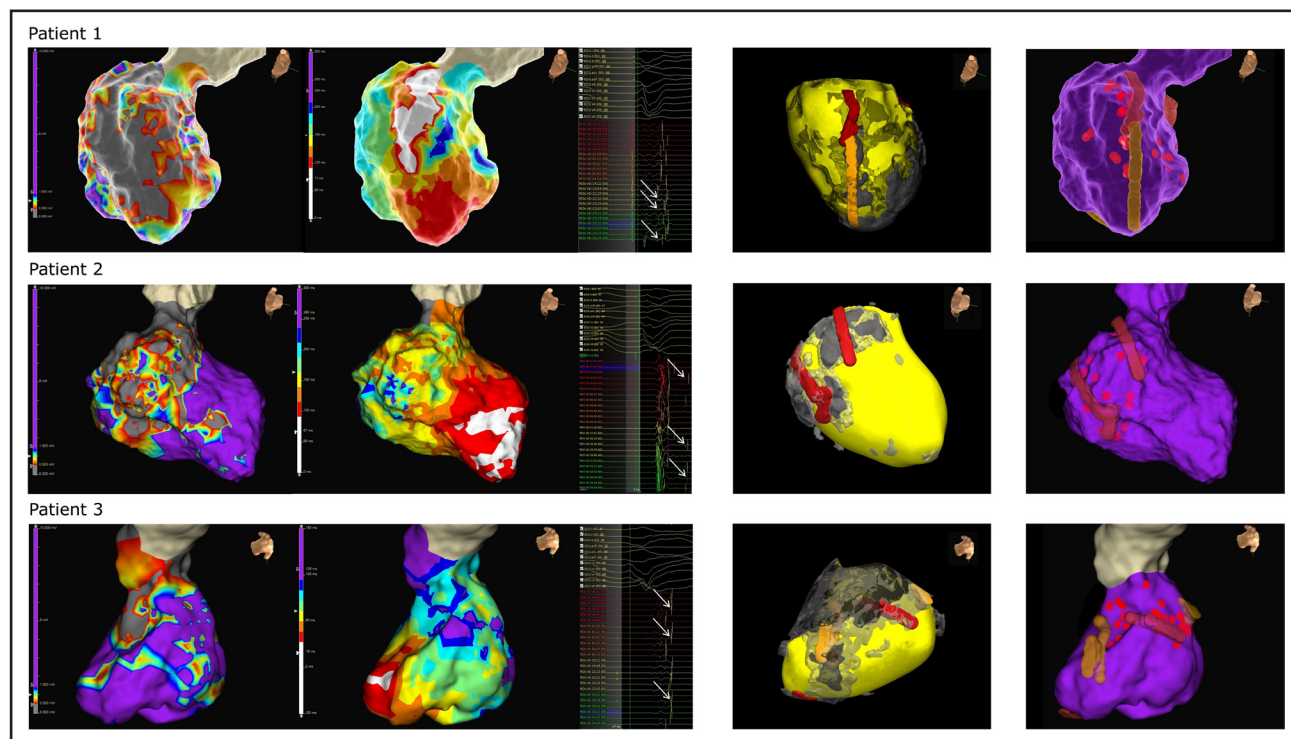


**Figure 3. Representative cases.**

Example cases from 3 patients who underwent invasive substrate mapping (left column), including voltage and activation mapping, with example abnormal electrograms displaying fractionation and late potentials (white arrows). Middle column shows the digital twin model with magnetic resonance imaging infarct (gray) and predicted sites (primary in red, secondary in orange). Right column shows final ablation lesion (red circles) set in comparison to the predicted sites.

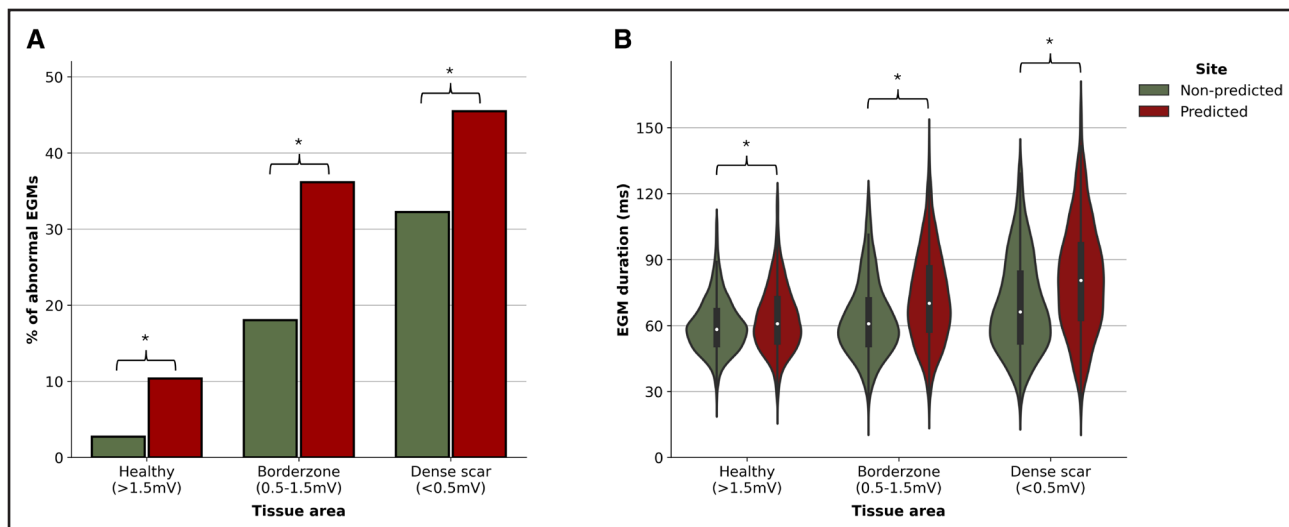


**Figure 4. Comparison of electrogram changes at digital twin-predicted versus nonpredicted sites.**

Comparison of prevalence of electrogram abnormalities (A) and electrogram (EGM) duration (B) between predicted and nonpredicted sites, stratified by tissue region. \*Statistical significance.

to show that this technology can be used regardless of pathogenesis to detect arrhythmogenic sites.

Substrate-based VT ablation relies on the identification of abnormal EGMs as a surrogate for the VT isthmus. Predicted sites from digital twins exhibited 41% greater frequency of EGM abnormalities compared with nonpredicted sites, therefore establishing their utility in guiding VT ablation. These abnormalities represent valid targets for substrate-based ablation and have been shown to correlate closely with the VT isthmus.<sup>38</sup> Furthermore, EGM duration was also prolonged at predicted sites compared with nonpredicted sites. EGM duration is known to predict the VT isthmus, with termination of the VT frequently achieved when the longest-duration EGMs are targeted.<sup>39</sup> The finding that a high proportion of DZs collocate to these predicted areas also underscores that the digital twin technology is capable of accurately detecting conduction slowing and isochronal crowding, which has emerged as a valid and effective approach to control VT.<sup>40,41</sup>

### EAM Low Voltage Versus MRI Scar: Which Is the Gold Standard?

Substrate-based VT ablation relies on accurate detection of myocardial scar followed by either complete scar homogenization or elimination of the abnormal EGMs within the scar.<sup>742</sup> Similarly, for heart digital twins to be effective, tissue characterization based on MRI signal intensity must accurately reflect the presence or absence of fibrotic tissue in the substrate. In our study, we showed a discrepancy in size between bipolar endocardial voltage-defined scar using conventional cutoff values and the MRI-derived scar, with the bipolar EAM underestimating the size of the scar. In contrast, the unipolar voltage map correlated more closely with the MRI-defined scar. Reasons for this include

the inability of bipolar mapping techniques to “visualize” epicardial or midmyocardial scar. Furthermore, traditional cutoff values of 1.5-mV bipolar voltage were derived from a small number of patients and confined to the ICM population, with the larger electrodes of ablation catheters used to acquire the data.<sup>43,44</sup> Another variable in MRI scar estimation is the variation in signal thresholding values that can be used during the creation of the digital twin. We show that, despite being labeled as “healthy” by bipolar voltage (>1.5 mV), there are still abnormalities in nearly 5% of EGMs. This was particularly true when the EGM was located within areas of MRI-defined scar. Therefore, it is highly likely that a personalized voltage cutoff is required

**Table 3. Comparison of Primary and Secondary Predicted Sites Within Low-Voltage Area (<1.5 mV)**

Parameter	Primary (n=1748)	Secondary (n=1074)	P value
Voltage			
Bipolar voltage, mV	0.72±0.39	0.71±0.41	0.26
EGM characteristics, n (%)			
Fractionation	573/1748 (32.8)	118/1074 (32.8)	1.0
Double potential	75/1748 (4.3)	23/1074 (2.1)	0.002
Late potential	103/1748 (5.9)	26/1074 (2.4)	<0.001
Other LAVA	178/1748 (10.2)	67/1074 (6.2)	<0.001
Any EGM abnormality	710/1748 (40.6)	406/1074 (37.8)	0.14
EGM timing, ms			
Onset	55.0±28.2	55.5±30.3	0.66
Offset	132.9±28.9	132.3±27.1	0.33
Duration	77.9±26.6	76.9±24.4	0.30
Offset to QRS offset	35.3±30.6	34.1±28.5	0.30

EGM indicates electrogram; and LAVA, local abnormal ventricular activity.

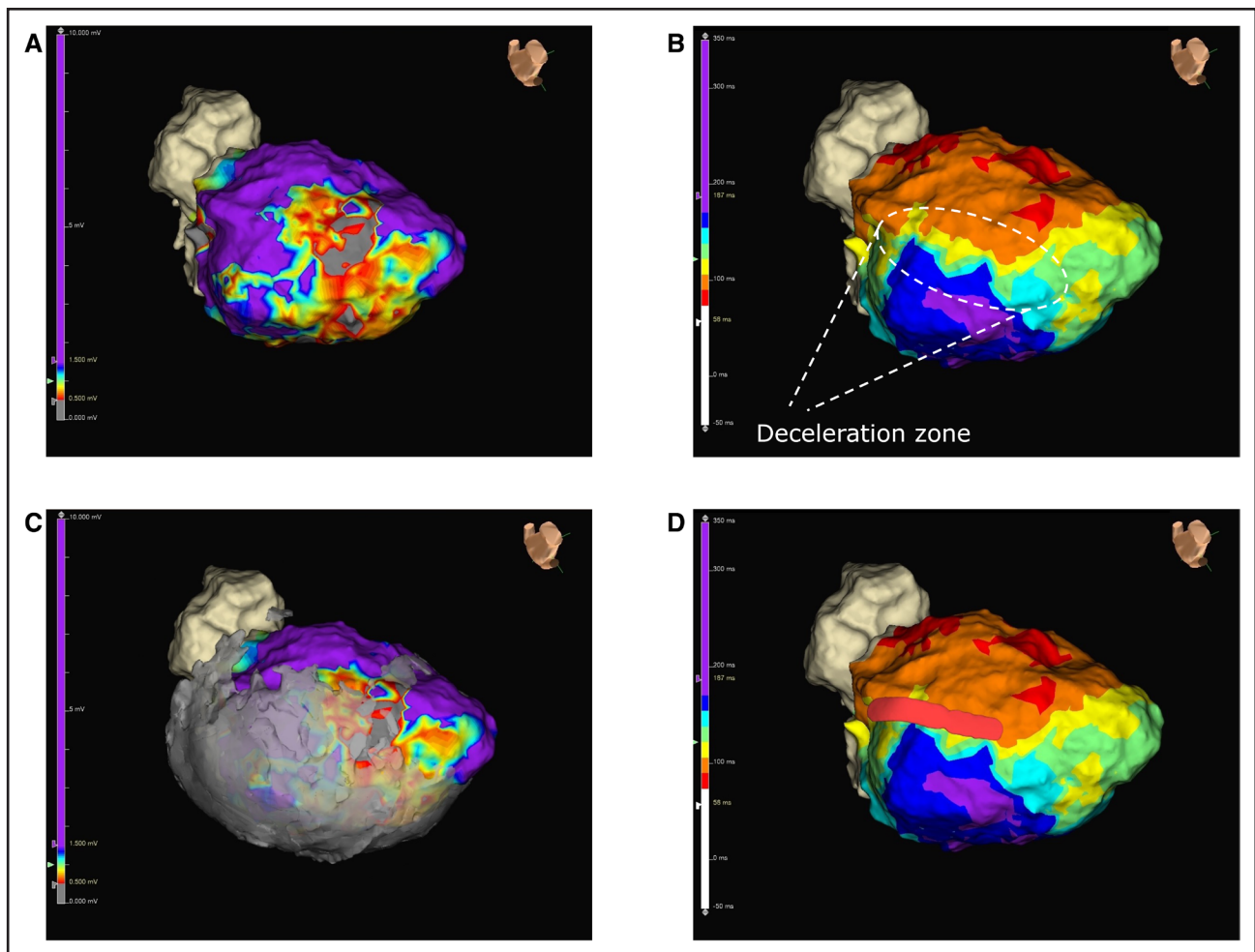


**Figure 5. Example of conduction slowing correctly predicted by the patient's digital twin.**

**A**, Substrate mapping revealed inferolateral wall scar. **B**, Isochronal late activation mapping demonstrated a deceleration zone (white oval). **C**, Voltage map with magnetic resonance imaging scar overlaid. **D**, Deceleration zone corresponds to a digital twin–predicted site on inferoseptal border of scar.

to define scar rather than a blanket value for all patients and all pathogeneses.

### Relative Importance of Primary Versus Secondary Sites in Predicting Substrate Abnormalities

More than one-third of patients undergoing VT ablation will require a repeat procedure at some stage.<sup>45</sup> Redo VT ablation is characterized by longer duration, greater technical difficulty, and higher complication rates compared with first-time ablation.<sup>45,46</sup> Heart digital twins have the unique advantage in predicting not only locations of critical importance to the VT circuit in the native substrate but also emergent locations in the new “landscape” (including scar plus lesions) and may therefore reduce the requirement for redo VT ablation. Our study is the first to compare the substrate characteristics between digital twin sites identified in the initial substrate and those identified after the application of a primary ablation lesion set.

Overall prevalence of EGM abnormalities and total EGM duration were similar between primary and secondary sites, and we postulate that the relatively small difference is seen because both sites are able to sustain VT under the right circumstances. Substrate abnormalities are arrhythmogenic but not sufficient in isolation for VT to occur. Functional components and stochastic events such as premature ventricular complexes are required to initiate and sustain a VT circuit. The identified secondary VTs require that a new area of block, generated by the primary ablation lesions, is present before a subsequent VT can occur. However, they still require the correct electrophysiological milieu to sustain a reentrant circuit.

### Implications for the Use of Digital Twins in Guiding VT Ablation

Heart digital twin technology takes advantage of a readily available preprocedural imaging modality to non-invasively predict the likely locations of a patient's VT.

Furthermore, it has the potential to determine the most efficient ablation strategy that will terminate all potential VT circuits a patient may harbor and can be used to help guide the need for epicardial access during VT ablation. By accurately predicting regions enriched with substrate abnormalities, a digital twin-guided substrate ablation may help avoid the requirement for VT induction and mapping, which can be time consuming and lead to hemodynamic instability. Furthermore, digital twins may allow an ablation strategy directly guided by the digital twin, without the need for comprehensive substrate mapping. Having a model before the procedure that provides guidance to the operator on where to focus to achieve rapid control of most reentrant circuits would lead to more manageable procedures with lower overall risk and duration. Furthermore, the total ablation area predicted by the digital twin is significantly smaller than the EAM- or MRI-detected scar area, implying that a digital twin-guided ablation would potentially result in a lower burden of ablation, again reducing procedural time and complication risk. Because of the iterative nature of the modeling process whereby simulations are repeated after application of the first set of ablation lesions to assess for the emergence of secondary VTs, this technology could also help reduce the requirement for repeat ablation, which is performed in an unacceptably high proportion of patients with VTA.

## Limitations

The heart digital twins described in this study are computationally expensive, requiring high-performance infrastructure and hours of simulation runs. However, efforts are underway to use artificial intelligence and other techniques to bring simulation times down to minutes or even seconds, thus rendering the technology scalable so that it can be used across centers. Accuracy of the models is dependent on obtaining high-quality LGE-CMR images, which can be challenging in the clinical environment and are particularly prone to artifact in patients with implantable cardioverter defibrillators, as demonstrated by the final recruitment rate of only 50% of screened patients. This issue is expected to be improved with more prevalent adoption of wideband imaging techniques and the integration of artificial intelligence into image segmentation. Our experience was that, as familiarity with the 3D LGE-CMR sequence improved throughout the study, the rates of acquiring adequate image quality improved significantly over time. Digital twin predictions also require validation in prospective studies of VT mapping and induction, which remain the current gold standard for VT ablation. These studies are in progress. Coregistration of the EAM with the MRI model was not automated and relied on expert approximation of the 2 surfaces. Small mismatches in surface coregistration could result in large discrepancies in the labeling of predicted and

unpredicted sites. Digital twin ablation lesions are assumed to be transmural with a uniform radius of 3.5 mm. This consistency is unlikely to be achieved clinically, and transmural is far from guaranteed, particularly in thick-walled structures such as the interventricular septum or LV summit.

## Conclusions

We present the first combined personalized computational and invasive electrophysiological study to validate the use of heart digital twins in predicting critical substrate abnormalities in scar-dependent VT. Digital twins represent a potential paradigm shift toward the application of personalized medicine in the treatment of arrhythmia. This study demonstrates their utility and accuracy in predicting the conventional invasive abnormalities targeted by modern substrate-based VT ablation. We expect that these findings will serve to increase the trust that clinicians place in this innovative technology and propel the mainstream use of digital twin-guided VT ablation.

## ARTICLE INFORMATION

Received May 30, 2024; accepted October 22, 2024.

### Affiliations

City St. George's, University of London, UK (M.C.W., A.C.L., M.M.S.). Alliance for Cardiovascular Diagnostic and Treatment Innovation, Johns Hopkins University, Baltimore, MD (M.C.W., A.P., N.A.T.). St. George's University Hospitals NHS Foundation Trust, London, UK (A.C.L., N.B., A.M., M.M.S.). Cleveland Clinic London, UK (M.M.S.).

### Sources of Funding

Dr Waight has received funding through the Advanced Ventricular Arrhythmia Training and Research Project, administered by the St. George's Hospital Charity (RES 20 21 001). Dr Trayanova has received grant funding from the National Institutes of Health (R01HL142496 and R01HL166759) and a grant from the Leducq Foundation. Drs Saba and Li have received modest, restricted grants from Abbott Laboratories.

### Disclosures

None.

### Supplemental Material

Methods  
Tables S1–S3  
Figures S1–S4  
References 47–52

## REFERENCES

1. Sapp JL, Wells GA, Parkash R, Stevenson WG, Blier L, Sarrazin J-F, Thibault B, Rivard L, Gula L, Leong-Sit P, et al. Ventricular tachycardia ablation versus escalation of antiarrhythmic drugs. *N Engl J Med*. 2016;375:111–121. doi: 10.1056/NEJMoa1513614
2. Reddy VY, Reynolds MR, Neuzil P, Richardson AW, Taborsky M, Jongnarangsin K, Kralovec S, Sediva L, Ruskin JN, Josephson ME. Prophylactic catheter ablation for the prevention of defibrillator therapy. *N Engl J Med*. 2007;357:2657–2665. doi: 10.1056/NEJMoa065457
3. Kuck K-H, Schaumann A, Eckardt L, Willems S, Ventura R, Delacrétaez E, Pitschner H-F, Kautzner J, Schumacher B, Hansen PS; VTACH Study Group. Catheter ablation of stable ventricular tachycardia before defibrillator implantation in patients with coronary heart disease (VTACH): a multicentre randomised controlled trial. *Lancet*. 2010;375:31–40. doi: 10.1016/S0140-6736(09)61755-4

4. Stevenson WG, Khan H, Sager P, Saxon LA, Middlekauff HR, Natterson PD, Wiener I. Identification of reentry circuit sites during catheter mapping and radiofrequency ablation of ventricular tachycardia late after myocardial infarction. *Circulation*. 1993;88:1647–1670. doi: 10.1161/01.cir.88.4.1647
5. Stevenson WG, Delacretaz E, Friedman PL, Ellison KE. Identification and ablation of macroreentrant ventricular tachycardia with the CARTO electroanatomical mapping system. *Pacing Clin Electrophysiol*. 1998;21:1448–1456. doi: 10.1111/j.1540-8159.1998.tb00217.x
6. Nakahara S, Tung R, Ramirez RJ, Gima J, Wiener I, Mahajan A, Boyle NG, Shivkumar K. Distribution of late potentials within infarct scars assessed by ultra high-density mapping. *Heart Rhythm*. 2010;7:1817–1824. doi: 10.1016/j.hrthm.2010.07.032
7. Jaïs P, Maury P, Khairy P, Sacher F, Nault I, Komatsu Y, Hocini M, Forclaz A, Jadidi AS, Weerasoorya R, et al. Elimination of local abnormal ventricular activities: a new end point for substrate modification in patients with scar-related ventricular tachycardia. *Circulation*. 2012;125:2184–2196. doi: 10.1161/CIRCULATIONAHA.111.043216
8. Di Biase L, Santangeli P, Burkhardt DJ, Bai R, Mohanty P, Carbuicchio C, Dello Russo A, Casella M, Mohanty S, Pump A, et al. Endo-epicardial homogenization of the scar versus limited substrate ablation for the treatment of electrical storms in patients with ischemic cardiomyopathy. *J Am Coll Cardiol*. 2012;60:132–141. doi: 10.1016/j.jacc.2012.03.044
9. Kuck KH, Tilz RR, Deneke T, Hoffmann BA, Ventura R, Hansen PS, Zarse M, Hohnloser SH, Kautzner J, Willems S; SMS Investigators. Impact of substrate modification by catheter ablation on implantable cardioverter-defibrillator interventions in patients with unstable ventricular arrhythmias and coronary artery disease: results from the multicenter randomized controlled SMS (Substrate Modification Study). *Circ Arrhythm Electrophysiol*. 2017;10:e004422. doi: 10.1161/CIRCEP.116.004422
10. Tung R, Xue Y, Chen M, Jiang C, Shatz DY, Besser SA, Hu H, Chung F-P, Nakahara S, Kim Y-H, et al; PAUSE-SCD Investigators. First-line catheter ablation of monomorphic ventricular tachycardia in cardiomyopathy concurrent with defibrillator implantation: the PAUSE-SCD randomized trial. *Circulation*. 2022;145:1839–1849. doi: 10.1161/CIRCULATIONAHA.122.060039
11. Della Bella P, Baratto F, Vergara P, Bertocchi P, Santamaria M, Notarstefano P, Calò L, Orsida D, Tomasi L, Piacenti M, et al. Does timing of ventricular tachycardia ablation affect prognosis in patients with an implantable cardioverter defibrillator? Results from the multicenter randomized PARTITA trial. *Circulation*. 2022;145:1829–1838. doi: 10.1161/CIRCULATIONAHA.122.059598
12. Willems S, Tilz RR, Steven D, Käääb S, Wegscheider K, Gellér L, Meyer C, Heeger C-H, Metzner A, Sinner MF, et al; BERLIN VT Investigators. Preventive or deferred ablation of ventricular tachycardia in patients with ischemic cardiomyopathy and implantable defibrillator (BERLIN VT). *Circulation*. 2020;141:1057–1067. doi: 10.1161/CIRCULATIONAHA.119.043400
13. Ding WY, Pearman CM, Bonnett L, Adlan A, Chin SH, Denham N, Modi S, Todd D, Hall MCS, Mahida S. Complication rates following ventricular tachycardia ablation in ischaemic and non-ischaemic cardiomyopathies: a systematic review. *J Interv Card Electrophysiol*. 2022;63:59–67. doi: 10.1007/s10840-021-00948-6
14. Yu R, Ma S, Tung R, Stevens S, Macias C, Bradfield J, Buch E, Vaseghi M, Fujimura O, Gornbein J, et al. Catheter ablation of scar-based ventricular tachycardia: Relationship of procedure duration to outcomes and hospital mortality. *Heart Rhythm*. 2015;12:86–94.
15. National Academies of Sciences Engineering and Medicine. Foundational research gaps and future directions for digital twins. 2024. Accessed April 12, 2024. <https://ncbin.nlm.nih.gov/books/NBK605507/>
16. Laubenbacher R, Mehrad B, Shmulevich I, Trayanova N. Digital twins in medicine. *Nat Comput Sci*. 2024;4:184–191. doi: 10.1038/s43588-024-00607-6
17. Trayanova N, Prakosa A. Up digital and personal: how heart digital twins can transform patient care. *Heart Rhythm*. 2024;21:89–99. doi: 10.1016/j.hrthm.2023.10.019
18. Shade JK, Prakosa A, Popescu DM, Yu R, Okada DR, Chrispin J, Trayanova NA. Predicting risk of sudden cardiac death in patients with cardiac sarcoidosis using multimodality imaging and personalized heart modeling in a multivariable classifier. *Sci Adv*. 2021;7:8020–8048.
19. O'hara RP, Binka E, Prakosa A, Zimmerman SL, Cartoski MJ, Abraham MR, Lu D-Y, Boyle PM, Trayanova NA. Personalized computational heart models with T1-mapped fibrotic remodeling predict sudden death risk in patients with hypertrophic cardiomyopathy. *eLife*. 2022;11:e73325. doi: 10.7554/eLife.73325
20. Arevalo HJ, Vadakkumpadan F, Guallar E, Jebb A, Malamas P, Wu KC, Trayanova NA. Arrhythmia risk stratification of patients after myocardial infarction using personalized heart models. *Nat Commun*. 2016;7:11437. doi: 10.1038/ncomms11437
21. Zhang Y, Zhang K, Prakosa A, James C, Zimmerman SL, Carrick R, Sung E, Gasperetti A, Tichnell C, Murray B, et al. Predicting ventricular tachycardia circuits in patients with arrhythmogenic right ventricular cardiomyopathy using genotype-specific heart digital twins. *eLife*. 2023;12:RP88865. doi: 10.7554/eLife.88865
22. Sung E, Prakosa A, Zhou S, Berger RD, Chrispin J, Nazarian S, Trayanova NA. Fat infiltration in the infarcted heart as a paradigm for ventricular arrhythmias. *Nat Cardiovasc Res*. 2022;1:933–945. doi: 10.1038/s44161-022-00133-6
23. Sung E, Prakosa A, Aronis KN, Zhou S, Zimmerman SL, Tandri H, Nazarian S, Berger RD, Chrispin J, Trayanova NA. Personalized digital-heart technology for ventricular tachycardia ablation targeting in hearts with infiltrating adiposity. *Circ Arrhythm Electrophysiol*. 2020;13:e008912. doi: 10.1161/CIRCEP.120.008912
24. Prakosa A, Arevalo HJ, Deng D, Boyle PM, Nikolov PP, Ashikaga H, Blauer JJE, Ghafoori E, Park CJ, Blake RC, et al. Personalized virtual-heart technology for guiding the ablation of infarct-related ventricular tachycardia. *Nat Biomed Eng*. 2018;2:732–740. doi: 10.1038/s41551-018-0282-2
25. Shade JK, Cartoski MJ, Nikolov P, Prakosa A, Doshi A, Binka E, Olivier L, Boyle PM, Spevak RJ, Trayanova NA. Ventricular arrhythmia risk prediction in repaired tetralogy of Fallot using personalized computational cardiac models. *Heart Rhythm*. 2020;17:408–414. doi: 10.1016/j.hrthm.2019.10.002
26. Prakosa A, Malamas P, Zhang S, Pashakhanloo F, Arevalo H, Herzka DA, Lardo A, Halperin H, McVeigh E, Trayanova N, et al. Methodology for image-based reconstruction of ventricular geometry for patient-specific modeling of cardiac electrophysiology. *Prog Biophys Mol Biol*. 2014;115:226–234. doi: 10.1016/j.pbmolbio.2014.08.009
27. Schmidt A, Azevedo CF, Cheng A, Gupta SN, Bluemke DA, Foo TK, Gerstenblith G, Weiss RG, Marbán E, Tomaselli GF, et al. Infarct tissue heterogeneity by magnetic resonance imaging identifies enhanced cardiac arrhythmia susceptibility in patients with left ventricular dysfunction. *Circulation*. 2007;115:2006–2014. doi: 10.1161/CIRCULATIONAHA.106.653568
28. Boyle PM, Ochs AR, Ali RL, Paliwal N, Trayanova NA. Characterizing the arrhythmogenic substrate in personalized models of atrial fibrillation: sensitivity to mesh resolution and pacing protocol in AF models. *Europace*. 2021;23:i3–i11. doi: 10.1093/europace/eaab385
29. Bayer JD, Blake RC, Plank G, Trayanova NA. A novel rule-based algorithm for assigning myocardial fiber orientation to computational heart models. *Ann Biomed Eng*. 2012;40:2243–2254. doi: 10.1007/s10439-012-0593-5
30. Ten Tusscher KHWJ, Noble D, Noble PJ, Panfilov AV. A model for human ventricular tissue. *Am J Physiol Heart Circ Physiol*. 2004;286:1573–1589. doi: 10.1152/ajpheart.00794.2003
31. Plank G, Loewe A, Neic A, Augustin C, Huang Y-L, Gsell MAF, Karabelas E, Nothstein M, Prassl AJ, Sánchez J, et al. The openCARP simulation environment for cardiac electrophysiology. *Comput Methods Programs Biomed*. 2021;208:106223. doi: 10.1016/j.cmpb.2021.106223
32. Battaglia A, Odille F, Magnin-Poull I, Sellal J-M, Hoyland P, Hooks D, Voilliot D, Felblinger J, de Chillou C. An efficient algorithm based on electrograms characteristics to identify ventricular tachycardia isthmus entrance in post-infarct patients. *Europace*. 2020;22:109–116. doi: 10.1093/europace/euz315
33. Chillou CD, Magnin-Poull I, Andronache M, Sacher F, Groben L, Abdelaal A, Muresan L, Jarmouni S, Schwartz J, Jaïs P, et al. Showing up channels for postinfarct ventricular tachycardia ablation. *PACE*. 2012;35:897–904. doi: 10.1111/j.1540-8159.2012.03429.x
34. Irie T, Yu R, Bradfield JS, Vaseghi M, Buch EF, Ajjjola O, Macias C, Fujimura O, Mandapati R, Boyle NG, et al. Relationship between sinus rhythm late activation zones and critical sites for scar-related ventricular tachycardia. *Circ Arrhythm Electrophysiol*. 2015;8:390–399. doi: 10.1161/CIRCEP.114.002637
35. Aziz Z, Shatz D, Raiman M, Upadhyay GA, Beaser AD, Besser SA, Shatz NA, Fu Z, Jiang R, Nishimura T, et al. Targeted ablation of ventricular tachycardia guided by wavefront discontinuities during sinus rhythm: a new functional substrate mapping strategy. *Circulation*. 2019;140:1383–1397. doi: 10.1161/CIRCULATIONAHA.119.042423
36. Roca-Luque I, Zaraket F, Garre P, Sanchez-Somonte P, Quinto L, Borrás R, Guasch E, Arbelo E, Tolosana JM, Brugada J, et al. Accuracy of standard bipolar amplitude voltage thresholds to identify late potential channels in ventricular tachycardia ablation. *J Interv Card Electrophysiol*. 2023;66:15–25. doi: 10.1007/s10840-022-01148-6
37. Hutchinson MD, Gerstenfeld EP, Desjardins B, Bala R, Riley MP, Garcia FC, Dixit S, Lin D, Tzou WS, Cooper JM, et al. Endocardial unipolar voltage

- mapping to detect epicardial ventricular tachycardia substrate in patients with nonischemic left ventricular cardiomyopathy. *Circ Arrhythm Electrophysiol.* 2011;4:49–55. doi: 10.1161/CIRCEP.110.959957
38. Zachariah D, Nakajima K, Rosario Limite L, Zweiker D, Spartalis M, Zirolia D, Musto M, D'Angelo G, Paglino G, Baratto F, et al. Significance of abnormal and late ventricular signals in ventricular tachycardia ablation of ischemic and nonischemic cardiomyopathies. *Heart Rhythm.* 2022;19:2075–2083. doi: 10.1016/j.hrthm.2022.08.008
  39. Rossi P, Cauti FM, Niscola M, Magnocavallo M, Polselli M, Capone S, Della Rocca DG, Rodriguez-Garrido J, Piccirillo G, Anguera I, et al. Ventricular electrograms duration map to detect ventricular arrhythmia substrate: the VEDUM Project Study. *Circ Arrhythm Electrophysiol.* 2023;16:447–455. doi: 10.1161/CIRCEP.122.011729
  40. von Alvensleben JC, Sandhu A, Nash D, Runciman DM, Schäfer M, Schaffer MS, Barrett C, Cerbin L, Tzou WS, Collins KK. MP-453092-5 isochronal late activation mapping for targeted ablation of ventricular tachycardia in patients with tetralogy of Fallot. *Heart Rhythm.* 2023;20:S130–S131. doi: 10.1016/j.hrthm.2023.03.468
  41. Uotani Y, Okubo Y, Komatsu Y, Nogami A, Aonuma K, Nakano Y. Isochronal late activation mapping of epicardial ventricular tachycardia in a patient with midventricular obstructive hypertrophic cardiomyopathy. *HeartRhythm Case Rep.* 2022;8:374–377. doi: 10.1016/j.hrcr.2022.03.001
  42. Gökoğlan Y, Mohanty S, Gianni C, Santangeli P, Trivedi C, Güneş MF, Bai R, Al-Ahmad A, Gallinhouse GJ, Horton R, et al. Scar homogenization versus limited-substrate ablation in patients with nonischemic cardiomyopathy and ventricular tachycardia. *J Am Coll Cardiol.* 2016;68:1990–1998. doi: 10.1016/j.jacc.2016.08.033
  43. Reddy VY, Wroblewski D, Houghtaling C, Josephson ME, Ruskin JN. Combined epicardial and endocardial electroanatomic mapping in a porcine model of healed myocardial infarction. *Circulation.* 2003;107:3236–3242. doi: 10.1161/01.CIR.0000074280.62478.E1
  44. Tschabrunn CM, Roujol S, Dorman NC, Nezafat R, Josephson ME, Anter E. High-resolution mapping of ventricular scar: comparison between single and multielectrode catheters. *Circ Arrhythm Electrophysiol.* 2016;9:e003841. doi: 10.1161/CIRCEP.115.003841
  45. Tzou WS, Tung R, Frankel DS, Di Biase L, Santangeli P, Vaseghi M, Bunch TJ, Weiss JP, Tholakanahalli VN, Lakkireddy D, et al. Outcomes after repeat ablation of ventricular tachycardia in structural heart disease: an analysis from the International VT Ablation Center Collaborative Group. *Heart Rhythm.* 2017;14:991–997. doi: 10.1016/j.hrthm.2017.03.008
  46. Garcia Garcia J, Arya A, Dinov B, Bollmann A, ter Bekke RMA, Vernooy K, Dagres N, Hindricks G, Darma A. Impact of repeat ablation of ventricular tachycardia in patients with structural heart disease. *Europace.* 2024;26:eoad367. doi: 10.1093/europace/eoad367
  47. Toussaint N, Mansi T, Delingette H, Ayache N, Sermesant M: An integrated platform for dynamic cardiac simulation and image processing: application to personalised tetralogy of Fallot simulation. In: EG VCBM 2008 - Eurographics Workshop on Visual Computing for Biomedicine. 2008:21–28.
  48. Bayer JD, Beaumont J, Krol A. Laplace–Dirichlet energy field specification for deformable models: an FEM approach to active contour fitting. *Ann Biomed Eng.* 2005;33:1175–1186. doi: 10.1007/s10439-005-5624-z
  49. Weiss DL, Seemann G, Keller DUJ, Farina D, Sachse FB, Dössel O. Modeling of heterogeneous electrophysiology in the human heart with respect to ECG genesis. *Comput Cardiol.* 2007:49–52. doi: 10.1109/cic.2007.4745418
  50. Yao JA, Hussain W, Patel P, Peters NS, Boyden PA, Wit AL. Remodeling of gap junctional channel function in epicardial border zone of healing canine infarcts. *Circ Res.* 2003;92:437–443. doi: 10.1161/01.RES.0000059301.81035.06
  51. Plank G, Zhou L, Greenstein JL, Cortassa S, Winslow RL, O'Rourke B, Trayanova NA. From mitochondrial ion channels to arrhythmias in the heart: computational techniques to bridge the spatio-temporal scales. *Philos Trans A Math Phys Eng Sci.* 2008;366:3381–3409. doi: 10.1098/rsta.2008.0112
  52. Bishop MJ, Rodriguez B, Qu F, Efimov IR, Gavaghan DJ, Trayanova NA. The role of photon scattering in optical signal distortion during arrhythmia and defibrillation. *Biophys J.* 2007;93:3714–3726. doi: 10.1529/biophysj.107.110981